T-probe: An Integrated Microscale Device for Online *in Situ* Single Cell Analysis and Metabolic Profiling Using Mass Spectrometry

Supporting Information

AUTHOR NAMES

*Renmeng Liu, Ning Pan, Yanlin Zhu, Zhibo Yang**

AUTHOR ADDRESS

Department of Chemistry and Biochemistry, University of Oklahoma, Norman, Oklahoma, 73019, USA

*Address reprint requests to Dr. Zhibo Yang, Department of Chemistry and Biochemistry, University of Oklahoma, Norman, Oklahoma 73019, USA

Tel: (405) 325-1772 Email: Zhibo.Yang@ou.edu

Table of Contents

Materials and Chemicals

Fabrication of T-probe. Fused silica capillaries (O.D. = 150.2 μm, I.D. = 74.7 μm, Polymicro Technologies, Phoenix, AZ). Laser-Based Micropipette Puller (P-2000, Sutter Instrument, Novato, CA). Polycarbonate slides (75 mm × 25 mm, P11011P; Science Supply Solutions, Elk Grove Village, IL, USA). Microscope slides (Fisherfinest, Waltham, MA). Computer numeric control (CNC) micro-engraver (CNC 3020, LiYang Welding Equipment Co., Ltd, Shenzhen, China). Micro-engraving bits (NJ3.1001, WeiTol Co., China). Micro electric cutting saw (Harbor Freight Tool, CA). Ultrasonic cleaner (model VGT-1860QT, GT Sonic Co., Guangdong, China). *Iso*-propanol (EMD Millipore Co., Billerica, MA). Bis[3-(trimethoxysilyl)propyl]amine (Bis-TPA) (Tokyo Chemical Industry Co., Tokyo, Japan). Ethyl alcohol (anhydrous, Pharmo-aaper, Brookfield, CT).

Cell Culture and Drug Treatment. Dulbecco's modified eagle's medium (DMEM) (Santa Cruz Biotechnology Inc. Dallas, TX). Fetal bovine serum (FBS) (Gibco by Life Technologies, Long Island, NY). Penicillin/streptomycin (Gibco, Life Technologies, Long Island, NY). Phosphate Buffered Saline (PBS) (Gibco by Life Technologies, Long Island, NY). 0.25% trypsin-EDTA (Gibco, Life Technologies, Long Island, NY). Dimethyl sulfoxide (DMSO) (>99.9%, MilliporeSigma Co. St. Louis, MO). Irinotecan hydrochloride (Alfa Aesar, Tewksbury, MA). Cell culture petri-dish (Greiner Bio-One North America Inc., Monroe, NC). 12-well plates (Cellstar, Greiner Bio-One North America Inc., Monroe, NC). 18 mm micro cover glass slide (VWR International, Radnor, PA).

SCMS Experiments. Manual XYZ-manipulator (M-MT-XYZ, Newport Co., Irvine, CA). Syringe pump (Nexus 3000, Chemyx Inc., Stafford, TX). Lateral microscope (Mustech Electronics Co., Hong Kong, China). Stereo microscope (Shenzhen D&F Co., China). Motorized XYZ-stage (MFA-CC, Newport Co., Irvine, CA). Conductive union (IDEX Health & Science LLC, Oak Harbor, WA). Thermo LTQ Orbitrap XL mass spectrometer (Thermo Fisher Scientific Inc., Waltham, MA). Methanol (UHPLC-MS, Fluka Analytical, Mexico City, Mexico). Water with 0.1% formic acid (LC/MS, Honeywell, Mexico City, Mexico). Irinotecan-d10 hydrochloride (Santa Cruz Biotechnology Inc. Dallas, TX). 1-oleoyl-2-palmitoyl-sn-glycero-3-phosphocholine (PC(18:1/16:0)) (Avanti Polar Lipids, Alabaster, AL). 1,3-dihexadecanoyl-2-(9Z-octadecenoyl)-glycerol (TG(16:0/18:1/16:0)) (Avanti Polar Lipids, Alabaster, AL). Leucine enkephalin (Millipore Sigma, St Louis, MO).

Software for SCMS Data Analysis. Xcalibur 3.0 (Thermo Fisher Scientific). Excel (Microsoft Co.). MetaboAnalyst (http://www.metaboanalyst.ca).[1] Geena 2 (http://bioinformatics.hsanmartino.it/geena2/).[2] Prism 7 (GraphPad Software).

SCMS Sample Preparation

HeLa is a mammalian cancer cell line that is widely used as a model system in biological and physiological research. In our study, HeLa cells were cultured under standard experimental conditions to ~80% confluence (~5 x 10^5 counts) in cell culture dish. Trypsinization was conducted to detach HeLa cells, followed by addition of complete Dulbecco's Modified Eagle's Medium (DMEM) containing 10% (v/v) fetal bovine serum (FBS) and 1% Pen-strep to quench trypsinization detachment and obtain cell suspension solution. 200 μL of cell suspension solution (containing ~10^3 cells) was seeded into an

individual well in a 12-well plate, in which a micro cover glass slide (18 mm in diameter) was placed onto the bottom of each well. 1.8 mL of complete DMEM solution was added into each well, and the 12-well plate with samples was kept in cell culture incubator (HERAcell, Thermo Scientific) under well controlled conditions (5% CO_2, 37 ºC, humidified). Cells were attached on the micro cover slide after being incubated for 18 h. To treat cells using anticancer drug, we dissolved drug compound (i.e., irinotecan) in dimethyl sulfoxide (DMSO) to prepare stock solutions, and dilute them into cell containing wells for different treatment concentrations. After treatment, cover slides containing cells were rinsed twice with fresh DMEM (without FBS) to remove residual molecules on cell surface prior to SCMS experiments. The untreated cells were incubated, rinsed, and analyzed as control in SCMS experiments. During the SCMS experiment, cells were submerged by DMEM solution to maintain their viability.

SCMS Data Analysis

Data acquired from the T-probe SCMS experiments were subjected to a comprehensive data analysis to gain biological insights into cellular response to drug treatment. In this work 9 and 11 cells in the control treatment groups, respectively, were analyzed, and their MS peaks were exported to an Excel spreadsheet. We then extracted the endogenous species (i.e., intracellular metabolites) from the data matrix by excluding MS peaks from exogenous species (i.e., DMEM solution and sampling solution) and instrument noise. Preserved endogenous species were subjected to peak normalization (to total ion current, TIC), peak alignment across multiple detected cells (using Geena 2), selection of common cellular species (>80% occurrence in all detected cells), and missing value imputation (using K-Nearest Neighbor algorithm).[3] The resulting datasets were subjected to mean-centering and Pareto scaling prior to OPLS-DA modeling (using MetaboAnalyst), and were subjected to log-transformation prior to follow-up statistical tests (using Prism 7). To evaluate model overfitting, we performed permutation tests for the established OPLS-DA model using MetaboAnalyst.

Tentative Labeling of Species Sensitively Reflecting Drug Treatment

In addition to utilizing the online metabolome database (METLIN and HMDB) to tentatively assign detected cellular species in control cells (Figure 3A, Table S1), we tentatively assign species with significantly changed abundance after drug treatment (as suggested by *t*-test *p*-values < 0.05). From our SCMS results, the ion signals of those drug-sensitive species were accompanied by other intracellular species such as PC(34:1), suggesting that they were endogenous cellular species (Figure S5). Based on accurate *m/z* values, isotopic distribution, and online database search, METLIN (https://metlin.scripps.edu) provides four potential candidates for the species with *m/z* 249.0640, including pyridoxamine-5'-phosphate (PMP), tazobactam, aprobarbital, and 2,6-dihydroxypseudooxynicotine (<5 ppm mass error). Tazobactam and aprobarbital are pharmaceutical drugs,[4-5] and 2,6-dihydroxypseudooxynicotine primarily presents in soil bacteria;[6] therefore, they are irrelevant to irinotecan metabolites and excluded. PMP is a precursor of pyridoxal-5'-phosphate (PLP), a coenzyme that actively participates in cellular metabolic activities;[7] therefor, it is a highly possible candidate for species with *m/z* 249.0640. For metabolite with *m/z* 686.0989, METLIN provides 2 possible labels, nicotinamide adenine dinucleotide (NAD) and fenugreekine. Knowing that fenugreekine is found

in the plant fenugreek,[8] whereas NAD a coenzyme widely existing in mammalian cells,[9] NAD is a highly possible candidate for species with *m/z* 686.0989. Combining such information with our earlier finding that those species are endogenous cellular species detected in individual cells with considerable S/N ratio, we assigned them with relatively high confidence, though we could not exclude the possibility that those metabolites remain completely unidentified up to now. To compare the change of abundance of PMP and NAD in control and irinotecan treatment groups, we provided the corresponding box plots (Figure 4B, inset). In addition, we demonstrated the receiver-operating characteristic (ROC) curve and calculated the area under curve (AUC) for both species (Figure S6). Our results showed considerable difference in terms of the abundance of species in the control group and drug treatment group (AUC = 0.79 for PMP and NAD, respectively). These results suggest that PMP and NAD could be potential indicators of cellular xenobiotic activities, especially at early treatment stage.

Supplementary Tables and Figures

Table S1. Tentative labeling of cellular species detected from singe HeLa cells in the control (no drug treatment) group.*

m/z	Tentative Labeling	Formula	Format	Δppm
203.066	Penmacric acid	$C_7H_{10}N_2O_5$	$[M + H]^+$	1
207.014	Oxalomalic Acid	$C_6H_6O_8$	$[M + H]^+$	2
207.051	DL-α-Lipoic Acid	$C_8H_{14}O_2S_2$	$[M + H]^+$	1
208.891	1,1,2-Trichloro-1,2,2-trifluoroethane	$C_2Cl_3F_3$	$[M + Na]^+$	0
210.017	3-methyl-2,5-dioxo-3-Pyrrolidineacetic acid	$C_7H_9NO_4$	$[M + K]^+$	3
213.075	L-Arginine	$C_6H_{14}N_4O_2$	$[M + K]^+$	0
220.009	Phosphoguanidinoacetate	$C_3H_8N_3O_5P$	$[M + Na]^+$	1
242.002	4-AMINO-3- (5-CHLOROTHIEN-2-YL)BUTANOIC ACID	$C_8H_{10}ClNO_2S$	$[M + Na]^+$	2
242.982	Phosphoramide mustard	$C_4H_{11}Cl_2N_2O_2P$	$[M + Na]^+$	3
249.036	Chorismic acid	$C_{10}H_{10}O_6$	$[M + Na]^+$	3
250.080	Deoxycytidine	$C_9H_{13}N_3O_4$	$[M + Na]^+$	0
251.981	3-Indoxyl phosphate	$C_8H_8NO_4P$	$[M + K]^+$	4
261.018	5-Methylthioribulose 1-phosphate	$C_6H_{13}O_7PS$	$[M + H]^+$	4
261.053	3-HYDROXYFLAVONE	$C_{15}H_{10}O_3$	$[M + Na]^+$	3
271.998	Dopamine 4-sulfate	$C_8H_{11}NO_5S$	$[M + K]^+$	3
276.014	5-Amino-4-chloro-2-(2,3-dihydroxyphenyl)-3(2H)-pyridazinone	$C_{10}H_8ClN_3O_3$	$[M + Na]^+$	2
281.067	Cysteinyl-Histidine	$C_9H_{14}N_4O_3S$	$[M + Na]^+$	3
284.990	(2E)-4-hydroxy-3-methylbut-2-en-1-yl trihydrogen diphosphate	$C_5H_{12}O_8P_2$	$[M + Na]^+$	0
287.035	EX-527	$C_{13}H_{13}ClN_2O$	$[M + K]^+$	0
291.093	2-p-Tolyl-5,6,7,8-tetrahydrobenzo[d]imidazo[2,1-b]thiazole	$C_{16}H_{16}N_2S$	$[M + Na]^+$	1
293.980	Sulbactam sodium	$C_8H_{10}NNaO_5S$	$[M + K]^+$	3
296.976	6-Phospho-g-gluconolactone	$C_6H_{11}O_9P$	$[M + K]^+$	4
303.037	5-(3,4-Dihydroxyphenyl)-5-ethylbarbituric acid	$C_{12}H_{12}N_2O_5$	$[M + K]^+$	2
307.020	Rhein	$C_{15}H_8O_6$	$[M + Na]^+$	4
309.017	Rhein-9-anthrone	$C_{15}H_{10}O_5$	$[M + K]^+$	3

318.970	Bis(4'-chlorophenyl)acetate	$C_{14}H_{10}Cl_2O_2$	$[M + K]^+$	3
321.135	10-Hydroxydesipramine	$C_{18}H_{22}N_2O$	$[M + K]^+$	4
330.101	8-Hydroxyamoxapine	$C_{17}H_{16}ClN_3O_2$	$[M + H]^+$	1
330.996	(±)-Mevalonic acid 5-pyrophosphate tetralithium salt	$C_6H_{14}O_{10}P_2$	$[M + Na]^+$	1
337.146	Steroid O-sulfate	$C_{18}H_{24}O_4S$	$[M + H]^+$	2
339.093	Promazine sulfoxide	$C_{17}H_{20}N_2OS$	$[M + K]^+$	0
339.989	2-(3,5-Dichlorophenylcarbamoyl)-1,2-dimethylcyclopropane-1-carboxylic acid	$C_{13}H_{13}Cl_2NO_3$	$[M + K]^+$	4
340.887	2,2',4,4',5-Pentachlorodiphenyl ether	$C_{12}H_5Cl_5O$	$[M + H]^+$	4
344.117	Arginyl-Methionine	$C_{11}H_{23}N_5O_3S$	$[M + K]^+$	4
351.258	Dihomo-g-Linolenic Acid-d6	$C_{20}H_{28}D_6O_2$	$[M + K]^+$	3
352.104	2,2'-(1-Phenyl-1H-1,2,4-triazole-3,5-diyl)bis-phenol	$C_{20}H_{15}N_3O_2$	$[M + Na]^+$	4
357.133	DEOXYSAPPANONE B 7,3'-DIMETHYL ETHER ACETATE	$C_{20}H_{20}O_6$	$[M + H]^+$	0
358.123	Aspartylglycosamine	$C_{12}H_{21}N_3O_8$	$[M + Na]^+$	2
359.010	8-Chloro-5,7,4'-trihydroxy-3-C-methylflavanone	$C_{16}H_{13}ClO_5$	$[M + K]^+$	4
359.092	5,7-Dihydroxyflavone 7-benzoate	$C_{22}H_{14}O_5$	$[M + H]^+$	1
359.128	Steroid O-sulfate		$[M + Na]^+$	2
361.008	2-hydroxy-4- (methylthio) butyric acid Calcium salt	$C_{10}H_{18}CaO_6S_2$	$[M + Na]^+$	4
361.075	L-Ascorbic acid-2-glucoside	$C_{12}H_{18}O_{11}$	$[M + Na]^+$	2
364.096	4'-Desmethylpapaverine	$C_{19}H_{19}NO_4$	$[M + K]^+$	3
364.936	ethyl-2-(2-pyridyl)-4-(bromomethyl)-Thiazole-5-Carboxylate	$C_{12}H_{11}BrN_2O_2S$	$[M + K]^+$	1
372.094	11-Hydroxy-11-isopropyl-4-methoxy-8-methyl-10,11-dihydro-6H-oxepino[2,3-d]pyrazino[1,2-a]pyrimidine-6,9(8H)-dione	$C_{16}H_{19}N_3O_5$	$[M + K]^+$	4
374.086	N-Acetylmuramic acid 6-phosphate	$C_{11}H_{20}NO_{11}P$	$[M + H]^+$	3
375.023	2,2-Bis(4-hydroxyphenyl)hexafluoropropane	$C_{15}H_{10}F_6O_2$	$[M + K]^+$	3
375.065	7-Hydroxymethyl-12-methylbenz[a]anthracene sulfate	$C_{20}H_{16}O_4S$	$[M + Na]^+$	3
377.070	Asn-Asn-OH	$C_{13}H_{14}N_4O_8$	$[M + Na]^+$	1
383.097	7-Hydroxy-2-methyl-4-oxo-4H-1-benzopyran-5-carboxylic acid 7-glucoside	$C_{17}H_{18}O_{10}$	$[M + H]^+$	0
387.046	1-Naphthoic acid glucuronide	$C_{17}H_{16}O_8$	$[M + K]^+$	4
388.036	m-Carboxyphenyl phenylacetamidomethylphosphonate	$C_{16}H_{16}NO_6P$	$[M + K]^+$	3
390.080	N-Acetyl-7-O-acetylneuraminic acid	$C_{11}H_{20}NO_{12}P$	$[M + K]^+$	0
391.117	5'-Demethoxydeoxypodophyllotoxin	$C_{21}H_{20}O_6$	$[M + Na]^+$	4
393.086	Abu-Phe4Cl-OH	$C_{18}H_{17}ClN_2O_6$	$[M + H]^+$	3
403.036	Radicicol	$C_{18}H_{17}ClO_6$	$[M + K]^+$	3
406.102	Ala-Trp-OH	$C_{19}H_{17}N_3O_6$	$[M + Na]^+$	2
415.002	beta-D-3-[5-Deoxy-5-(dimethylarsinyl)ribofuranosyloxy]-2-hydroxy-1-propanesulfonic acid	$C_{10}H_{21}AsO_9S$	$[M + Na]^+$	1
416.085	CAY10571	$C_{21}H_{16}FN_3O_2S$	$[M + Na]^+$	2
422.065	Fenoterol sulfate		$[M + K]^+$	4

424.116	3-Piperidinemethanol, 4-(4-fluorophenyl)-, (3S,4R)-glucuronide	$C_{17}H_{21}NO_7S$	$[M + K]^+$	1
427.080	5-Hydroxy-7,2',3',4',5'-pentamethoxyflavone	$C_{20}H_{20}O_8$	$[M + K]^+$	2
429.125	15-HydroxyCyproterone	$C_{22}H_{27}ClO_4$	$[M + K]^+$	4
431.060	Ser-Phe4Cl-OH	$C_{18}H_{17}ClN_2O_7$	$[M + Na]^+$	3
431.096	3-(a-Naphthoxy)lactic acid glucuronide	$C_{19}H_{20}O_{10}$	$[M + Na]^+$	2
435.123	Met-TyrMe-OH	$C_{20}H_{22}N_2O_7S$	$[M + H]^+$	2
441.063	N-(4-Chloro-3-methyl-5-isothiazolyl)-N-methyl-2-[p-[(alpha,alpha,alpha-trifluoro-p-tolyl)oxy]phenyl]acetamide	$C_{20}H_{16}ClF_3N_2O_2S$	$[M + H]^+$	3
445.037	Methyl 18,18-dibromo-17-octadecen-5,7-diynoate	$C_{19}H_{26}Br_2O_2$	$[M + H]^+$	0
445.995	O-Desmethyltolrestat sulfate	$C_{15}H_{12}F_3NO_6S_2$	$[M + Na]^+$	0
460.029	Asn-Phe4Cl-OH	$C_{18}H_{16}ClN_3O_7$	$[M + K]^+$	2
466.064	Asp-Trp-OH	$C_{20}H_{17}N_3O_8$	$[M + K]^+$	1
473.086	4'-Hydroxyfenoprofen glucuronide		$[M + K]^+$	3
487.041	2,3-Dihydro-5,5',7,7'-tetrahydroxy-2-(4-hydroxyphenyl)[3,8'-bi-4H-1-benzopyran]-4,4'-dione	$C_{24}H_{16}O_9$	$[M + K]^+$	3
493.082	Nap-Met-OH	$C_{23}H_{22}N_2O_6S$	$[M + K]^+$	2
495.079	8-Hydroxytricetin 7-glucuronide	$C_{21}H_{18}O_{14}$	$[M + H]^+$	4
507.154	HoPhe-Nap-OH	$C_{28}H_{24}N_2O_6$	$[M + Na]^+$	2
513.045	Chicoric acid	$C_{22}H_{18}O_{12}$	$[M + K]^+$	3
517.987	6-[(1S,2R)-1,2-Dihydroxy-3-triphosphooxypropyl]-7,8-dihydropterin	$C_9H_{16}N_5O_{13}P_3$	$[M + Na]^+$	3
519.091	Torachrysone 8-(6-oxalylglucoside)	$C_{22}H_{24}O_{12}$	$[M + K]^+$	2
541.139	3-CHLORO-8β-HYDROXYCARAPIN, 3,8-HEMIACETAL	$C_{27}H_{31}ClO_7$	$[M + K]^+$	0
563.990	Formamidopyrimidine nucleoside triphosphate	$C_{10}H_{18}N_5O_{15}P_3$	$[M + Na]^+$	0
567.021	Orientin 7-O-sulfate	$C_{21}H_{20}O_{14}S$	$[M + K]^+$	0
583.016	8-Hydroxyluteolin 8-glucoside-3'-sulfate	$C_{21}H_{20}O_{15}S$	$[M + K]^+$	0
613.988	m-Hydroxydiphenyldimercury(1+)	$C_{12}H_{11}Hg_2O$	$[M + K]^+$	4
621.139	Epicatechin 3-O-(2-trans-cinnamoyl-beta-D-allopyranoside)	$C_{30}H_{30}O_{12}$	$[M + K]^+$	3
645.559	CE(16:1)	$C_{43}H_{74}O_2$	$[M + Na]^+$	1
647.574	CE(16:0)	$C_{43}H_{76}O_2$	$[M + Na]^+$	0
669.082	Isorhamnetin 3-(6'-galloylglucoside)	$C_{29}H_{26}O_{16}$	$[M + K]^+$	4
671.574	CE(20:5)	$C_{47}H_{74}O_2$	$[M + H]^+$	3
673.590	CE(18:1)	$C_{45}H_{78}O_2$	$[M + Na]^+$	0
695.574	CE(20:4)	$C_{47}H_{76}O_2$	$[M + Na]^+$	0
712.066	Adenophostin B	$C_{18}H_{28}N_5O_{19}P_3$	$[M + H]^+$	0
719.574	CE(22:6)	$C_{49}H_{76}O_2$	$[M + Na]^+$	0
725.558	PE-Cer(d37:1)	$C_{39}H_{79}N_2O_6P$	$[M + Na]^+$	1
727.564	PA(O-37:0)	$C_{40}H_{81}O_7P$	$[M + Na]^+$	1
739.053	Molybdopterin guanine dinucleotide	$C_{20}H_{24}N_{10}O_{13}P_2S_2$	$[M + H]^+$	2
754.536	PE(37:4)	$C_{42}H_{76}NO_8P$	$[M + H]^+$	2
756.552	PC(32:0)	$C_{40}H_{78}NO_8P$	$[M + Na]^+$	2
768.589	PC(O-34:1)	$C_{44}H_{82}NO_7P$	$[M + Na]^+$	1
780.552	PC(34:2)	$C_{42}H_{80}NO_8P$	$[M + Na]^+$	4
782.568	PC(34:1)	$C_{42}H_{82}NO_8P$	$[M + Na]^+$	1

799.679	TG(46:1)	$C_{49}H_{92}O_6$	$[M + Na]^+$	0
804.549	PC(36:4)	$C_{44}H_{80}NO_8P$	$[M + Na]^+$	3
808.584	PC(36:2)	$C_{44}H_{84}NO_8P$	$[M + Na]^+$	1
810.600	PC(36:1)	$C_{44}H_{86}NO_8P$	$[M + Na]^+$	2
813.695	TG(49:4)	$C_{52}H_{92}O_6$	$[M + H]^+$	2
825.695	TG(50:5)	$C_{53}H_{92}O_6$	$[M + H]^+$	2
827.711	TG(50:4)	$C_{53}H_{94}O_6$	$[M + H]^+$	1
830.568	PC(40:8)	$C_{48}H_{80}NO_8P$	$[M + H]^+$	3
832.584	PC(40:7)	$C_{48}H_{82}NO_8P$	$[M + H]^+$	1
834.600	PC(38:3)	$C_{46}H_{86}NO_8P$	$[M + Na]^+$	2
843.706	20:0-Glc-Cholesterol	$C_{53}H_{94}O_7$	$[M + H]^+$	1
853.727	TG(52:5)	$C_{55}H_{96}O_6$	$[M + H]^+$	1
855.743	TG(52:4)	$C_{55}H_{98}O_6$	$[M + H]^+$	0
856.583	PE(43:6)	$C_{48}H_{84}NO_8P$	$[M + Na]^+$	1
858.600	PC(40:5)	$C_{48}H_{86}NO_8P$	$[M + Na]^+$	3
881.758	TG(54:5)	$C_{57}H_{100}O_6$	$[M + H]^+$	1

**: CE = cholesteryl ester*
PA = phosphtatidic acid
PC = phosphatidylcholine
PE = phosphatidylethanolamide
TG = triglyceride

Table S2. Cellular species significantly altered by anticancer drug irinotecan treatment (1 μM for 1 hr).*

Identifier	*m/z*	*t*-test *p*-value	Fold Change
1	213.075	0.035064	-1.46
2	221.031	0.039181	-1.626
3	244.871	0.049922	-1.686
4	249.061	0.019267	1.421
5	309.017	0.04285	-1.823
6	402.948	0.016886	-2.116
7	432.045	0.022224	1.342
8	450.068	0.04054	1.532
9	458.031	0.049733	1.308
10	466.064	0.034084	1.415
11	472.047	0.049008	1.26
12	572.965	0.040449	1.322
13	574.963	0.009845	1.335
14	652.111	0.005891	1.417
15	654.108	0.008264	1.422
16	686.095	0.028517	1.22
17	737.056	0.035396	1.264

**: All acquired SCMS data sets were subjected to generalized log-transformation prior to two sample t-test.*

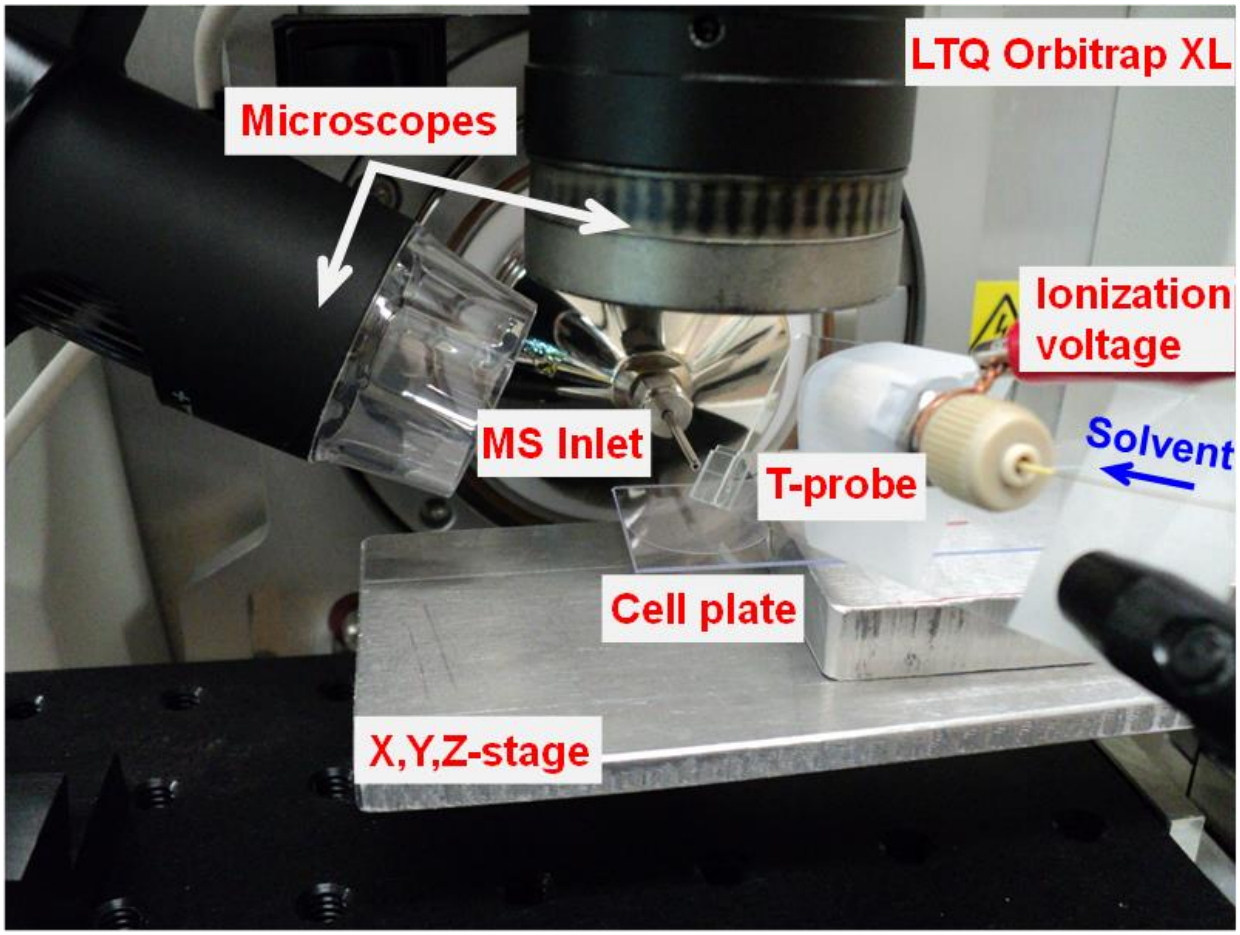

Figure S1. In-house developed SCMS platform for online and *in situ* analysis of live single cells using the T-probe.

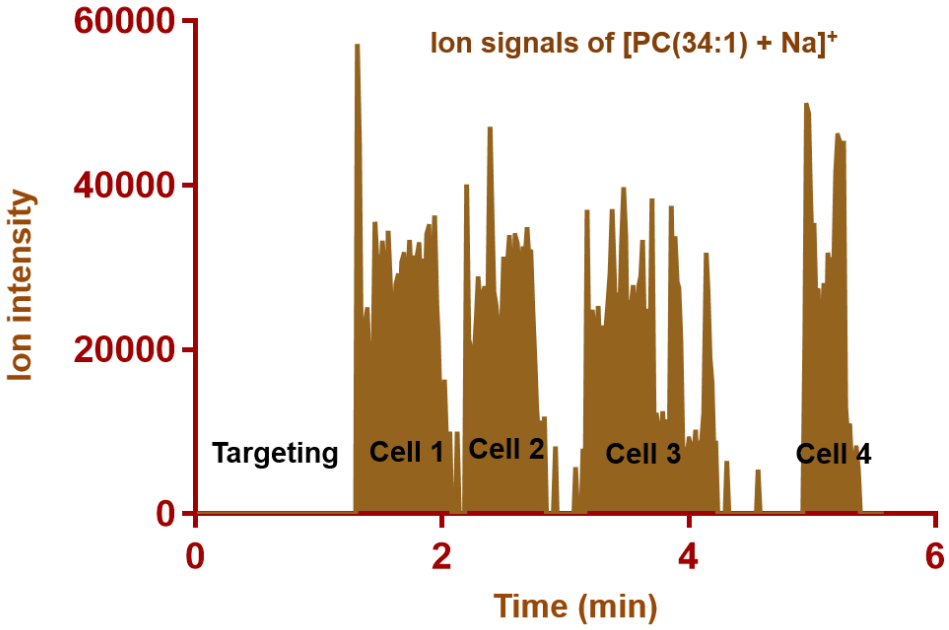

Figure S2. Successive SCMS detection of an intracellular species, [PC(34:1) + $Na]^+$, from multiple single cells using one T-probe.

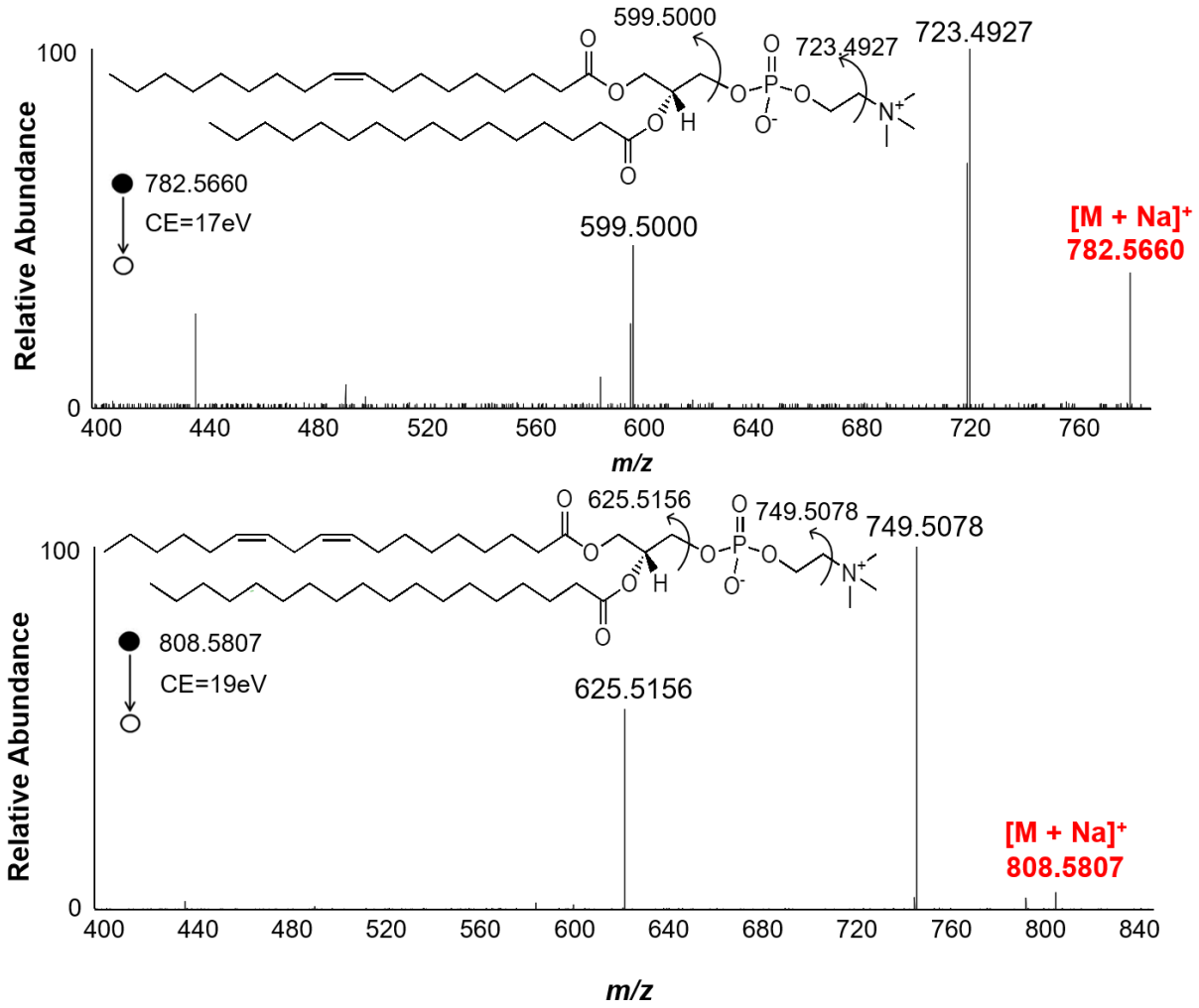

Figure S3. Online MS/MS spectra of $[PC(34:1) + Na]^+$ (top) and $[PC(36:2) + Na]^+$ (bottom) obtained at single cell level. CE: collision energy.

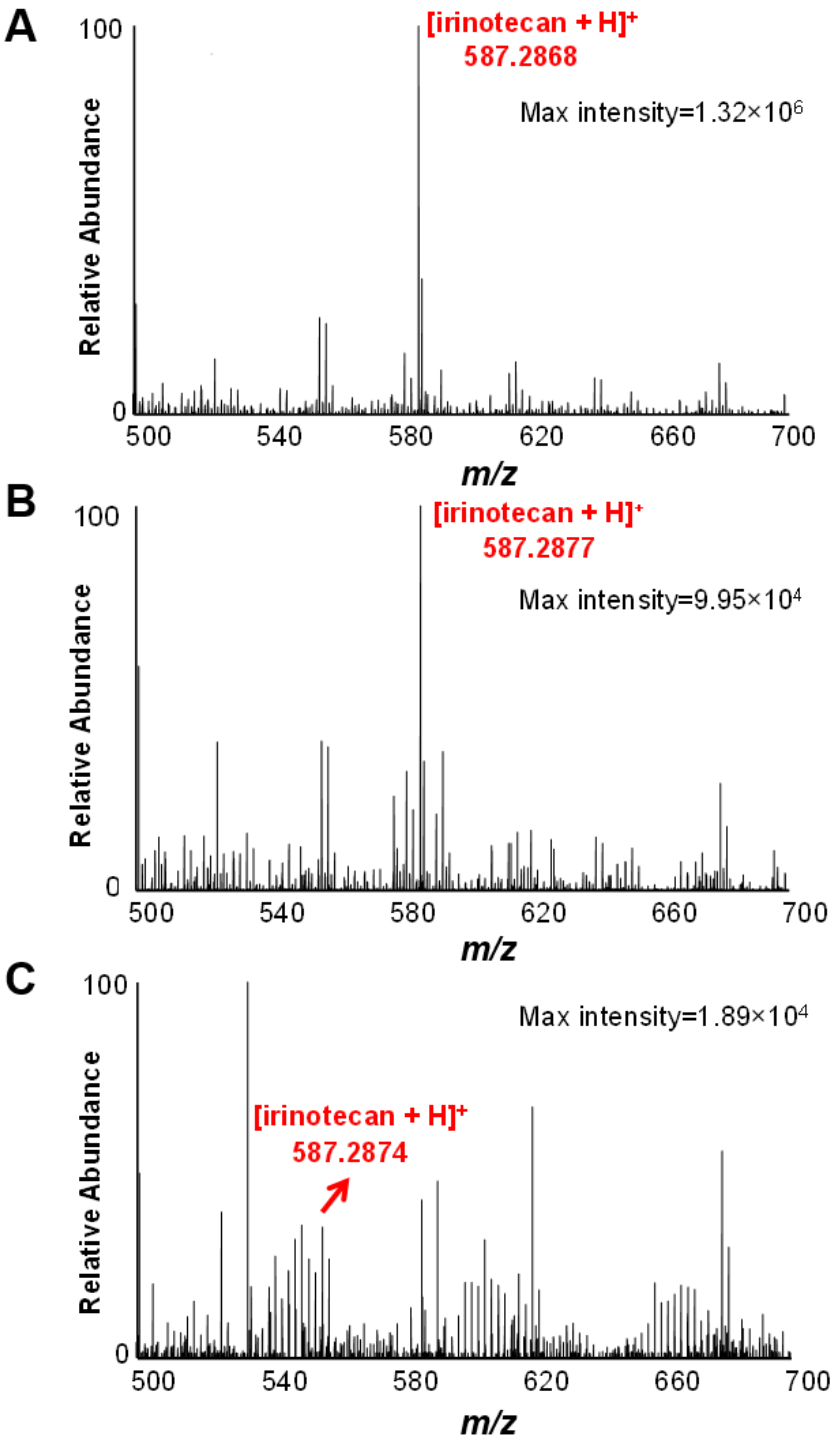

Figure S4. The drug target, [irinotecan + H]$^+$, can be detected from single cells under a series of treatment conditions including (A) 10 µM, (B) 1 µM, and (C) 100 nM for 1 h.

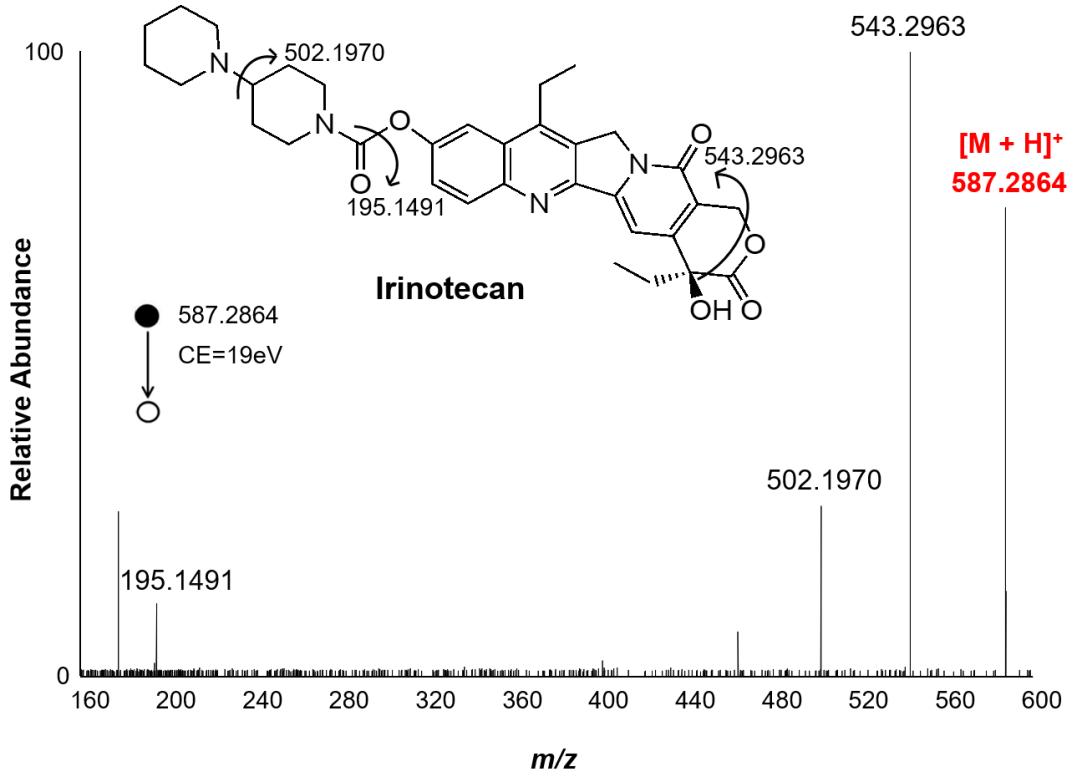

Figure S5. Online MS/MS spectrum of the drug target, [Irinotecan + H]$^+$, obtained at single cell level. CE: collision energy.

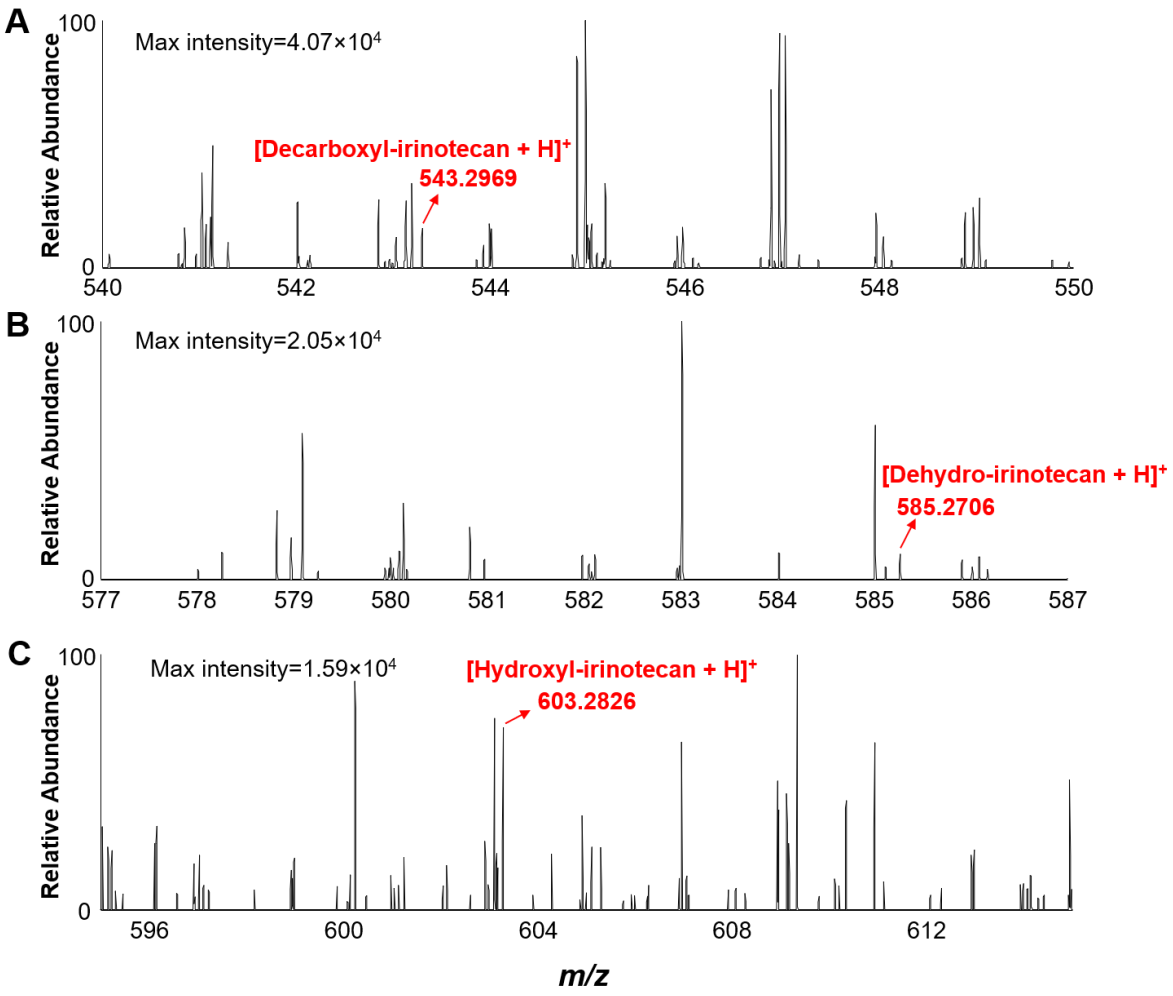

Figure S6. SCMS detections of irinotecan metabolites, including (A) decarboxyl-irinotecan, (B) dehydro-irinotecan, and (C) hydroxyl-irinotecan from single cells treated with 10 μM irinotecan for 1 h.

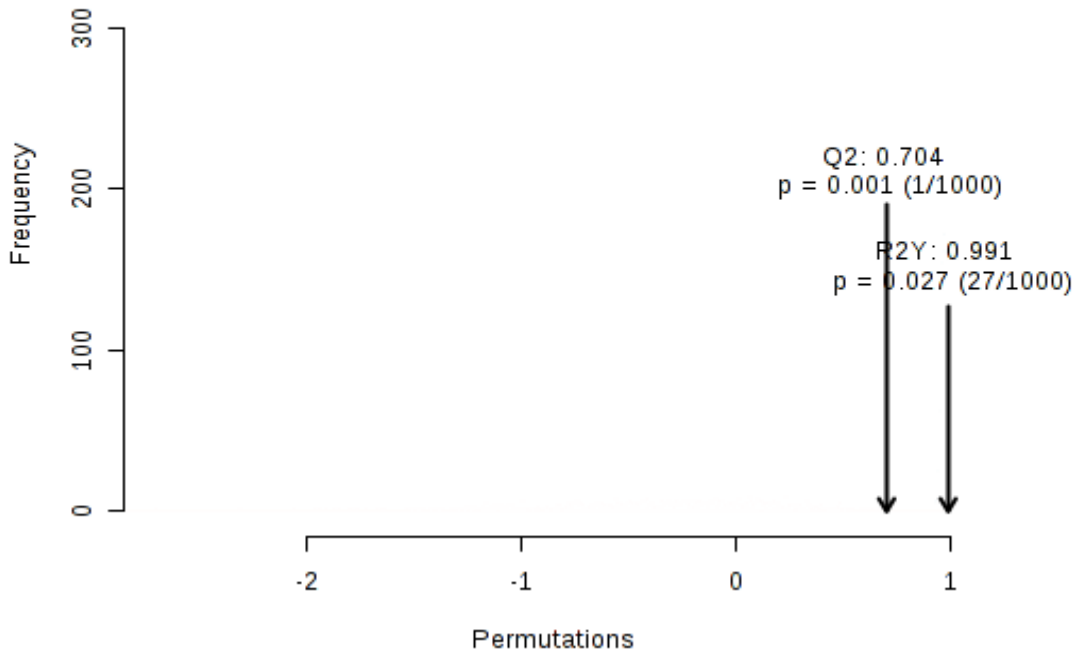

Figure S7. Evaluation of the overfitting potential of the OPLS-DA model using permutation test. The observed Q^2 (p = 0.001) and R^2Y (p = 0.027) are significantly different from the permuted values.

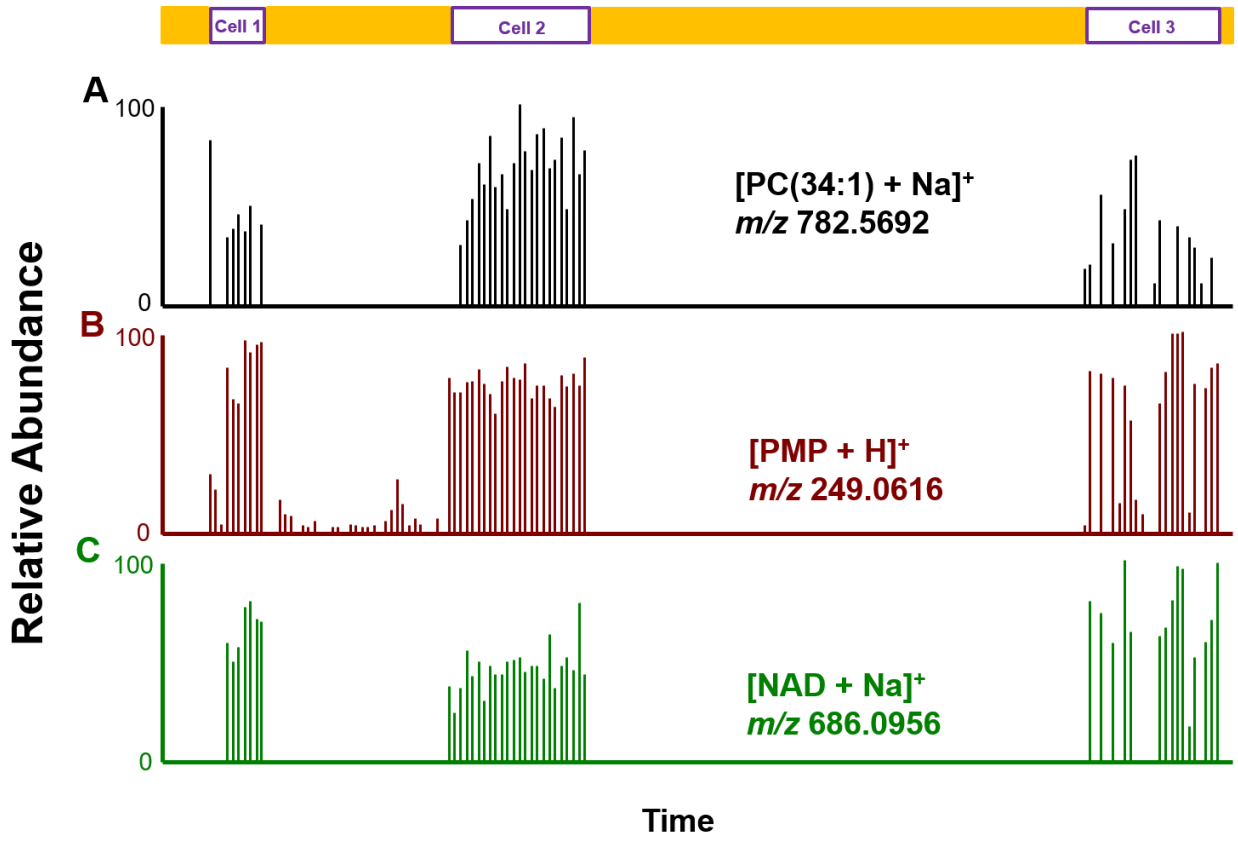

Figure S8. Simultaneous detection of three endogenous cellular species such as (A) PC(34:1) (confirmed by online MS/MS analysis), (B) PMP (tentatively assigned), and (C) NAD (tentatively assigned) in three different single cells. Their ion signals appeared and disappeared within the same time frame.

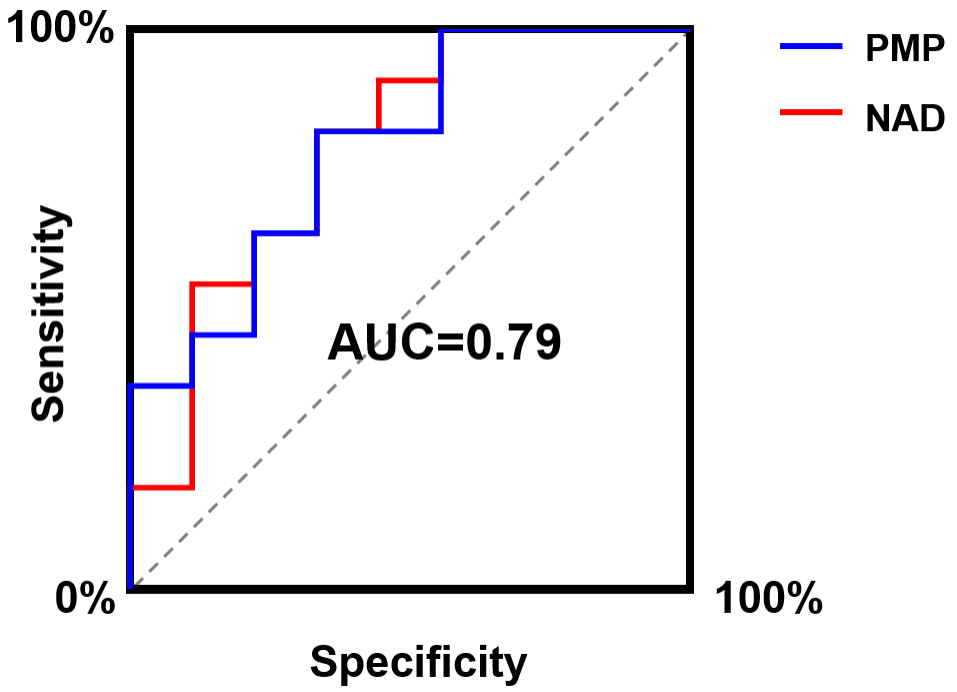

Figure S9. Receiver-operating characteristic (ROC) curve was generated corresponding to true positive rate (sensitivity) *versus* false positive rate (specificity) for PMP (blue line) and NAD (red line), respectively. Both species demonstrated considerable change of abundance after drug treatment (1 μM irinotecan for 1h), as area under (AUC) curve reached 0.79 for both species.

Reference

(1) Xia, J.; Sinelnikov, I. V.; Han, B.; Wishart, D. S., MetaboAnalyst 3.0—making metabolomics more meaningful. *Nucleic Acids Res.* **2015,** *43* (W1), W251-W257.
(2) Romano, P.; Profumo, A.; Rocco, M.; Mangerini, R.; Ferri, F.; Facchiano, A., Geena 2, improved automated analysis of MALDI/TOF mass spectra. *BMC Bioinformatics* **2016,** *17* (Suppl 4), 61.
(3) Di Guida, R.; Engel, J.; Allwood, J. W.; Weber, R. J. M.; Jones, M. R.; Sommer, U.; Viant, M. R.; Dunn, W. B., Non-targeted UHPLC-MS metabolomic data processing methods: a comparative investigation of normalisation, missing value imputation, transformation and scaling. *Metabolomics* **2016,** *12* (5), 93.
(4) Shah, P. J.; Ryzner, K. L., Evaluating the Appropriate Use of Piperacillin/Tazobactam in a Community Health System: A Retrospective Chart Review. *P&T* **2013,** *38* (8), 462-483.
(5) Klaunig, J. E.; Kamendulis, L. M.; Yong, X., Epigenetic mechanisms of chemical carcinogenesis. *Human & Experimental Toxicology* **2000,** *19* (10), 543-555.
(6) Chiribau, C. B.; Sandu, C.; Fraaije, M.; Schiltz, E.; Brandsch, R., A novel γ-N-methylaminobutyrate demethylating oxidase involved in catabolism of the tobacco alkaloid nicotine by Arthrobacter nicotinovorans pAO1. *Eur. J. Biochem.* **2004,** *271* (23-24), 4677-4684.
(7) Galluzzi, L.; Vacchelli, E.; Michels, J.; Garcia, P.; Kepp, O.; Senovilla, L.; Vitale, I.; Kroemer, G., Effects of vitamin B6 metabolism on oncogenesis, tumor progression and therapeutic responses. *Oncogene* **2013,** *32* (42), 4995-5004.
(8) Ghosal, S.; Srivastava, R. S.; Chatterjee, D. C.; Dutta, S. K., Fenugreekine, a new steroidal sapogenin-peptide ester of Trigonella foenum-graecum. *Phytochemistry* **1974,** *13* (10), 2247-2251.
(9) Billington, R. A.; Travelli, C.; Ercolano, E.; Galli, U.; Roman, C. B.; Grolla, A. A.; Canonico, P. L.; Condorelli, F.; Genazzani, A. A., Characterization of NAD uptake in mammalian cells. *J. Biol. Chem.* **2008,** *283* (10), 6367-6374.